Electronic Supplementary Material (ESI) for Journal of Materials Chemistry A.

Supporting Information

Synergistic Effect of Three-dimensional Orchid-like TiO_2 Nanowire Networks and Plasmonic Nanoparticles for Highly Efficient Mesoscopic Perovskite Solar Cells

*Haejun Yu, Jongmin Roh, Juyoung Yun and Jyongsik Jang**

[*] Prof. Jyongsik Jang

School of Chemical and Biological Engineering,
Seoul National University, 599 Gwanangno, Gwanakgu, Seoul 151-742, Korea
E-mail: jsjang@plaza.snu.ac.kr
Tel.: +82-2-880-7069
Fax: +82-2-880-1604

Measurement *of Roughness factor*.

The films based on TiO_2 NP and OC-TiO_2 NW were prepared with commercial and home-made paste which was dissolved in anhydrous ethanol (1:3 weight ratio). The TiO_2 solution were deposited by spin-coating, followed by annealing at 500 °C in furnace. The OC-TiO_2 NW-based film was post-treated with 20 mM of aqueous $TiCl_4$ and annealed at 500 °C in furnace. The resulting films were immersed in an ethanol-based dye solution (N719, 1.262×10^{-4} M) and kept at room temperature for 18 h. After dyeing, the films were rinsed with distilled water and dried at 80 °C oven for 20 min. For desorption of dye-molecule on TiO_2 films, the films were immersed in 5 mL of 0.01 M NaOH solution, followed by measuring UV-Vis absorbance with the desorbed dye solution. In extremely low concentration, the UV-Vis absorbance follows *Beer-Lambert law*.

Beer-Lambert law

$$A = \varepsilon \cdot b \cdot C, \quad C = A / \varepsilon \cdot b$$

ε : absorptivity [L/g·cm] or [mol·cm]

b : path length [cm]

C : concentration [mol/L]

The absorptivity of N719 dye is 1.47×10^{4} $L \cdot mol^{-1} \cdot cm^{-1}$ at 535 nm in literature.[2] The path length of cuvette is 1 cm. The concentration of reference dye solution was 1.262×10^{-4} M, and it was used for obtaining an extinction coefficient (absorptivity) of N719 as an experimental value. Through measurement of UV-Vis absorbance of reference dye solution, the value of 1.26×10^{4} $L \cdot mol^{-1} \cdot cm^{-1}$ at 535 nm was obtained as an experiment extinction coefficient of the dye. Because the concentration of initial dye solution and desorbed dye solution was extremely low, the Beer-lambert law can be applied in this measurement.

The concentration for TiO_2 NP and OC-TiO_2 NW-based film was measured by UV-Vis absorption and *Beer-lambert law equation*. The number of dye molecule was measured by multiplying Avogadro's number with each mole-number. The NaOH solution (5 mL) was used for dye desorption from TiO_2-based film. The real surface area was measured by multiplying the surface area of dye molecule with the number of desorbed dye molecules. The each dye molecule has a surface area of 1.65 nm^2.[3,4]

Finally, roughness factor of two samples can be calculated from the following formula.

$$Roughness\ factor\ = \frac{Real\ surface\ area}{Geometric\ surface\ area}$$

$$= \frac{Desorbed\ dye\ absorbance\ \times\ Avogadro\ number\ x\ Area\ of\ single\ N719\ dye}{Absorptivity\ (\varepsilon) \times path\ length\ (b)\ \times Geometric\ surface\ area}$$

The geometric surface area (projected area) was 5 cm^2

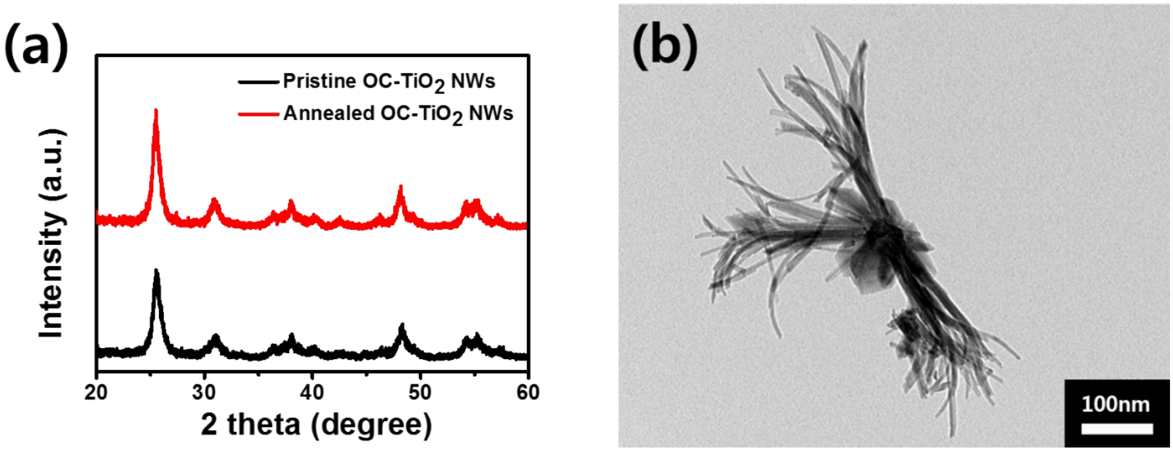

Fig. S1. (a) X-ray diffraction (XRD) patterns of pristine OC–TiO_2 NWs and OC–TiO_2 NWs annealed at 500 °C. (b) TEM image of OC–TiO_2 NWs after annealing.

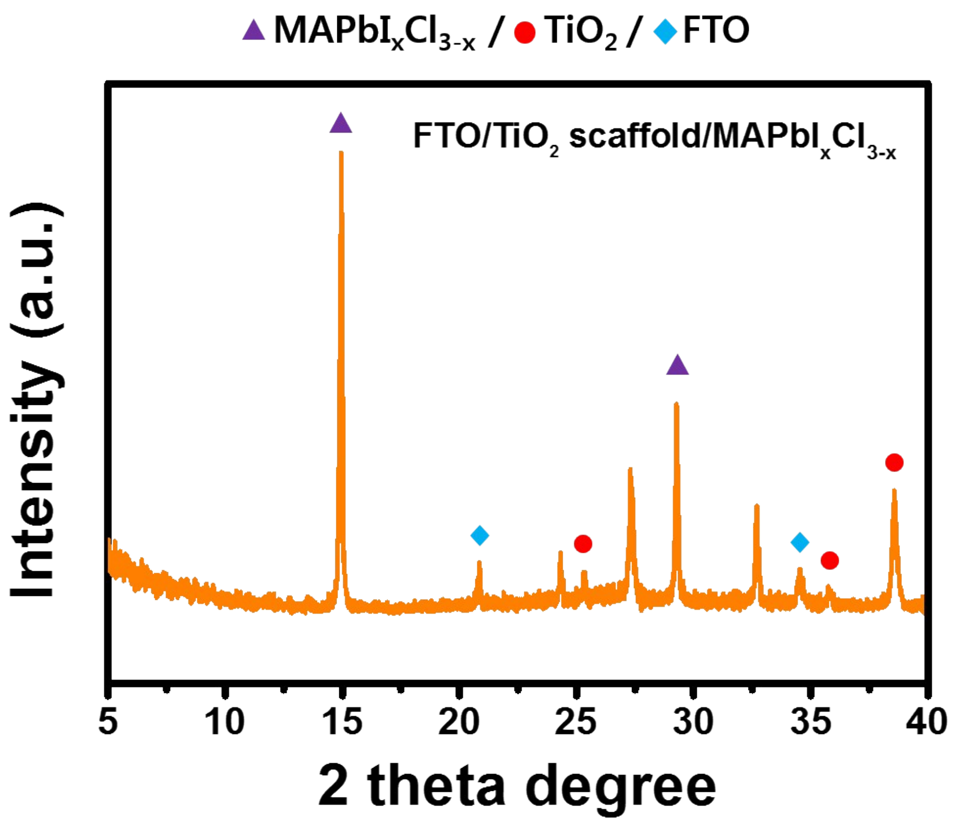

Fig. S2. XRD pattern of the perovskite deposited on the FTO/TiO$_2$ ETL.

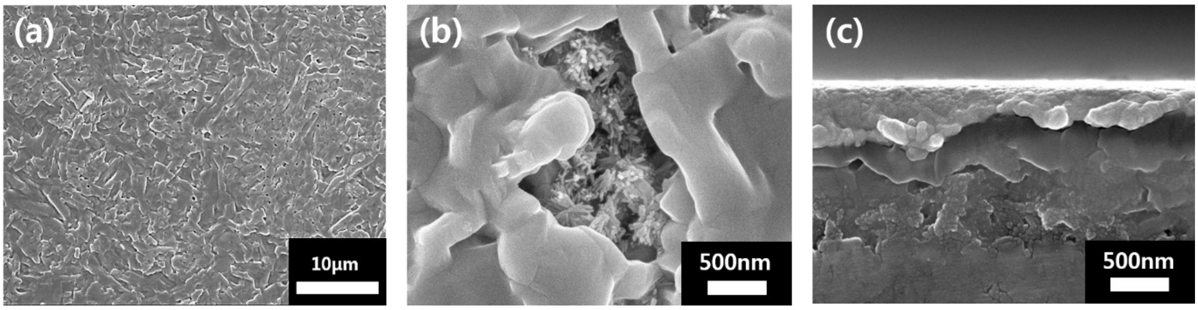

Fig. S3. SEM images showing (a) high coverage of the surface by the perovskite, (b) OC–TiO_2 NWs under the perovskite and (c) a cross-sectional view of the OC–TiO_2 NW-based ETL.

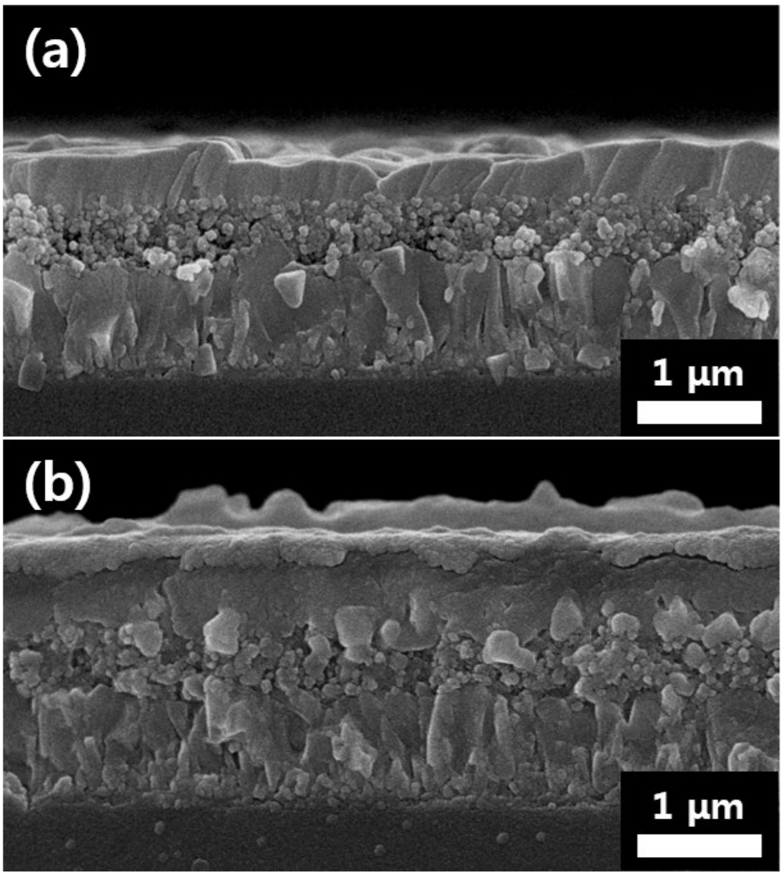

Fig. S4. SEM image displaying a cross-sectional view of (a) a TiO_2 NPs/perovskite layer and (b) a complete PSC based on TiO_2 NPs scaffold layer. The perovskite could not penetrate into the bottom of substrate perfectly due to cramped TiO_2 NPs structure.

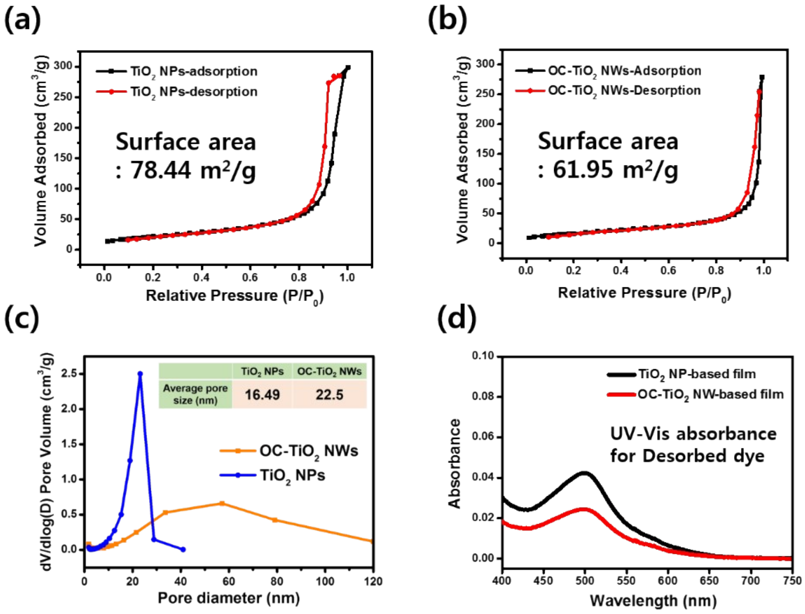

Fig. S5. (a) BET analysis of the TiO_2 NPs and (b) OC-TiO_2 NWs for specific surface area measurement. (c) BJH pore size distribution of TiO_2 NPs and OC-TiO_2 NWs. The average pore size is 16.49 nm and 22.50 nm for TiO_2 NPs and OC-TiO_2 NWs respectively. (d) UV-vis absorbance spectra of the desorbed dye from each TiO_2 films for obtaining a roughness factor of two films.

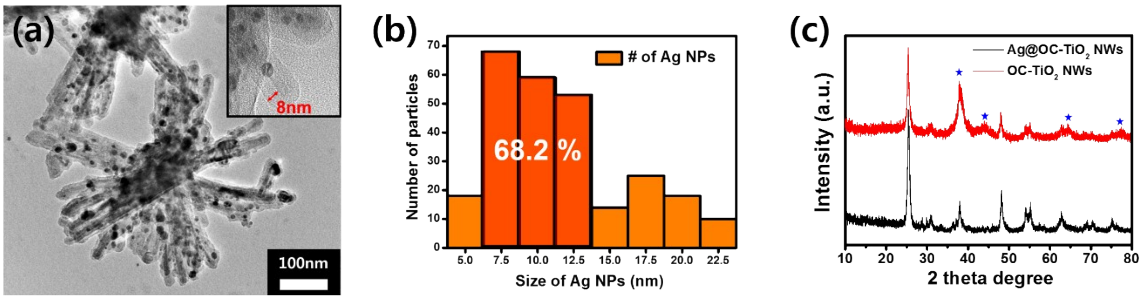

Fig. S6. (a) TEM image of the SiO_2@Ag@OC–TiO_2 NWs. (b) Histogram of the size for Ag NPs embedded in OC-TiO_2 NW. (c) XRD pattern of the Ag@OC–TiO_2 NWs and OC–TiO_2 NWs. The asterisks indicate the characteristic peaks for the Ag NPs.

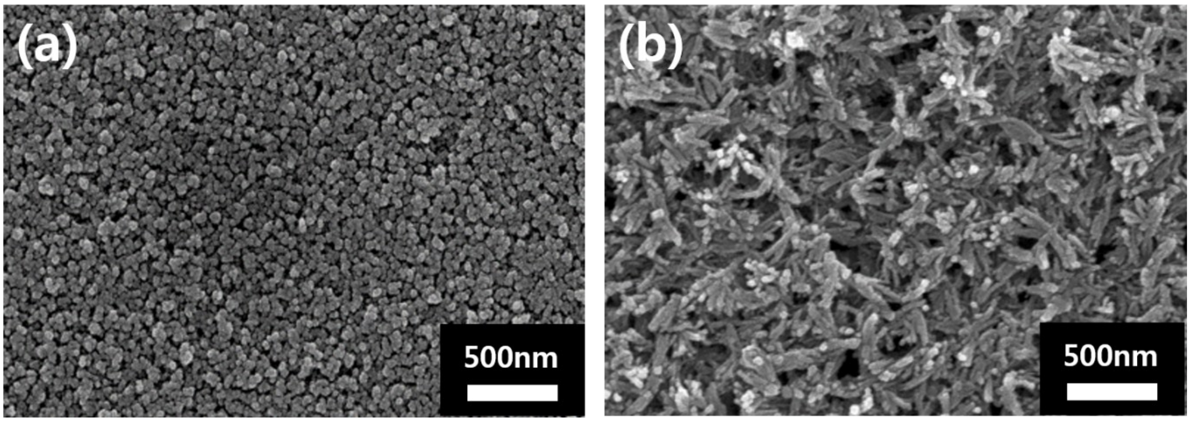

Fig. S7. SEM images of (a) TiO_2 NPs and (b) OC–TiO_2 NWs. The pore size increased when the NPs were replaced with NWs.

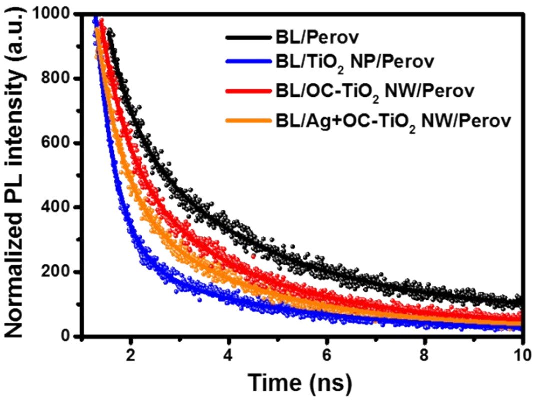

Fig. S8. Time-resolved PL spectra of $MAPbI_xCl_{3-x}$ films deposited on scaffold layers consisting of TiO_2 NPs, OC–TiO_2 NWs or Ag/OC–TiO_2 NWs. The fitted curves were obtained by a bi-exponential decay equation.

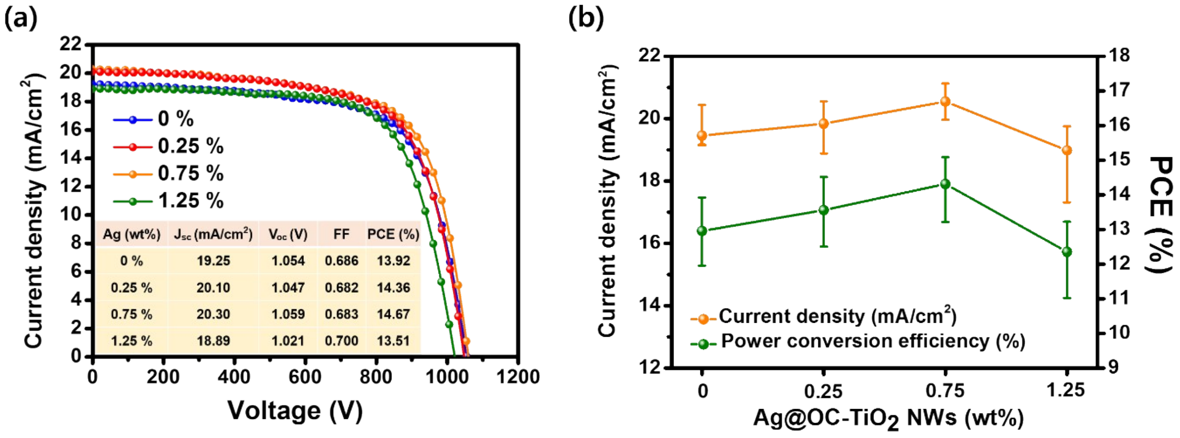

Ag (wt%)	J_{sc} (mA/cm^2)	V_{oc} (V)	FF	PCE (%)
0 %	19.25	1.054	0.686	13.92
0.25 %	20.10	1.047	0.682	14.36
0.75 %	20.30	1.059	0.683	14.67
1.25 %	18.89	1.021	0.700	13.51

Fig. S9. (a) J–V curves of OC–TiO$_2$ NW-based PSCs as a function of the weight ratio of Ag NPs (0–1.25 %). (b) Short-circuit current (green line) and PCE (orange line) as a function of the weight ratio of Ag NPs. The average parameters were obtained from 10 devices for each condition.

Table S1. Summary of BET analysis for TiO_2 NP-based film and OC-TiO_2 NW-based film.

Film of ETL	*Specific surface area* (m^2/g)	*Average pore size* (nm)
TiO_2 NPs	78.44	16.49
OC-TiO_2 NWs	61.95	22.50

Table S2. Summary of roughness factor measurement for TiO2 NP-based film and OC-TiO2 NW-based film according as an experimental or literature absorptivity value. The geometric surface area (projected area) was 5 cm^2.

	TiO_2 NPs	OC-TiO_2 NWs
Concentration (M) (experiment absorptivity)	1.91×10^{-5}	1.13×10^{-5}
Concentration (M) (absorptivity in literature)	1.64×10^{-5}	0.97×10^{-5}
# of desorbed dye molecule (experiment absorptivity)	5.75×10^{16}	3.40×10^{16}
# of desorbed dye molecule (absorptivity in literature)	4.93×10^{16}	2.92×10^{16}
Real surface area (m^2) (experiment absorptivity)	0.0949	0.0561
Real surface area (m^2) (absorptivity in literature)	0.0813	0.0482
Roughness factor (R_f) (experiment absorptivity)	189.8	162.6
Roughness factor (R_f) (absorptivity in literature)	111.2	96.4

Table S3. Average photovoltaic performance parameters obtained for 9 PSC devices measured under 100 mW cm^{-2} simulated AM1.5G illumination. Effect of $TiCl_4$ treatment (20 mM) on PSCs based on OC-TiO_2 NWs scaffold layer.

	J_{sc} (mA·cm^{-2})	V_{oc} (V)	*FF*	η_{avg} (%)
$TiCl_4$ (X)	18.72	0.939	0.629	11.08
$TiCl_4$ (O)	20.27	1.009	0.664	13.57

Table S4. Average photovoltaic performance parameters obtained for 20 PSC devices measured under 100 mW cm^{-2} simulated AM1.5G illumination. Three different kinds of TiO_2 were used as ETLs: TiO_2 NPs, OC–TiO_2 NWs and Ag/OC–TiO_2 NWs.

ETL for device	J_{sc} (mA cm^{-2})	V_{oc} (V)	*FF*	η_{avg} (%)	η_{max} (%)
TiO_2 NPs	18.82 ± 0.84	1.011 ± 20.4	0.639 ± 0.02	12.17 ± 0.89	13.10
OC–TiO_2 NWs	19.44 ± 0.41	1.020 ± 21.8	0.654 ± 0.03	12.97 ± 0.63	14.03
Ag/OC-TiO_2 NWs	20.46 ± 0.38	1.040 ± 19.3	0.666 ± 0.03	14.18 ± 0.60	15.05

ETL, electron transport layer; $J_{sc,}$ short-circuit current density; V_{oc}, open-circuit voltage; FF, fill factor; TiO_2 NPs, TiO_2 nanoparticles; OC–TiO_2 NWs, orchid-like TiO_2 nanowires, Ag/OC–TiO_2 NWs; Mixture of SiO_2@Ag@OC–TiO_2 NWs and OC–TiO_2 NWs